

Fast drift Alfvén waves excited at the low-frequency band in tokamak plasmas

A. G. Elfimov and C. J. A. Pires

Institute of Physics, University of São Paulo, 05508-900 São Paulo, Brazil

R. M. O. Galvão

Institute of Physics, University of São Paulo, 05508-900 São Paulo, Brazil and Centro Brasileiro de Pesquisas em Física, Rio de Janeiro 22290-180, Brazil

(Received 27 June 2007; accepted 17 September 2007; published online 29 October 2007)

It is shown that fast drift Alfvén waves can be excited in tokamak plasmas by an external antenna operating in the low-frequency band. The dispersion of these waves depends on the derivative of the q -profile or drift terms in the case of low or negative shear. The wave absorption is determined by the Alfvén continuum dissipation and has an oscillating increase with frequency. Typical global Alfvén wave resonances are found at the plasma core for different signs of poloidal/toroidal mode numbers ($N/M < 0$) for a standard tokamak safety factor profile with central value $q_0 > 1$. © 2007 American Institute of Physics. [DOI: 10.1063/1.2801414]

Drift effects on tokamak plasma stability and transport have been actively discussed for more than 40 years. A series of theoretical works related to drift waves were recently reviewed in Refs. 1 and 2. The main result of the investigations is that plasma transport is controlled mainly by low-frequency (LF) drift turbulence. In the last decade, some mechanisms to control the anomalous transport have been discovered.³ One of them is the reversed magnetic field shear configurations, which help to suppress turbulence in the plasma core and to create an internal transport barrier.⁴ The LF magnetic fields have also been proposed⁵ to generate a chaotic magnetic layer at the plasma edge, to control heat and particle transport. In the TEXTOR (Torus Experiment for Technology Oriented Research), the fields in the 1–10 kHz band are driven by the dynamic ergodic divertor⁶ (DED) to actuate on the plasma at the rational magnetic surface $q=3$. The LF fields driven by the DED have mainly magnetic components, but they also have the potential to excite a drift eigenmode spectrum. Recently, cylindrical multifluid codes^{7–9} have been used to analyze the penetration of LF fields into the TEXTOR plasma. In the models used, the LF fields are driven by helical coils with current, i.e., $j_{\theta,z} = \sum_{MN} J_{\theta,zM,N} \delta(r-b) \exp[i(M\theta + Nz/R_0 - \omega t)]$, where M and N are poloidal and toroidal wave numbers, respectively. It was shown that these fields can strongly dissipate at the Alfvén wave (AW) continuum, which is described by the dispersion relation $(\omega^2/c^2)\epsilon_{11} = k_{\parallel}^2$, where ω is the angular frequency, ϵ_{11} is a radial component of the plasma dielectric tensor, k_{\parallel} is the parallel wave vector, and c is the speed of light. The AW continuum is formed by mode conversion into the quasialelectrostatic Alfvén wave (QEAW), $k_r^2 = [(\omega^2/c^2)\epsilon_{11} - k_{\parallel}^2]\epsilon_{33}/\epsilon_{11}$, if the QEAW dissipation is sufficiently strong due to electron-ion collisions, or Landau damping in the parallel component of the ϵ_{33} -tensor component.

Here, we incorporate the drift effects^{1,9–11} into the cylindrical code⁷ and calculate LF fields and absorption induced by helical coils for different mode numbers (M/N) in the LF band, below the band with possible excitation of toroidicity

induced Alfvén eigenmodes for TEXTOR plasma parameters with standard, “flat,” and negative shear.

To proceed with tensor calculations for magnetized plasmas, we use equilibrium Maxwell distribution F_M with shifted parallel velocity V_{α} of the species in the velocity space $(v_{\perp}, \sigma, v_{\parallel})$ corrected with the drift effect,^{1,9,11} $F_d \sin \sigma = (v_{\perp}/\omega_c)(\partial F_M/\partial r) \sin \sigma$. The perturbed distribution function is represented⁹ as one wave mode expanded in Fourier series over σ -angle $\tilde{F} = (f_0 + f_1 \cos \sigma + f_2 \sin \sigma) \exp[i(M\theta + k_z z - \omega t)]$, and three terms of the distribution are used for the calculations in the first Larmor radius approximation. In equations for the $f_{1,2}$ components, the collisional integral is used in Krook form ($\nu_{ef} = \nu_e = 2.91 \times 10^{-6} n_e \ln \Lambda / T_e^{3/2}$ for electrons and $\nu_{ef} = \nu_i = \nu_e m_e / m_i$ for ions),

$$i(k_{\parallel} v_{\parallel} - \omega) f_1 - \omega_c f_2 + \frac{e}{m} E_1 \left(\frac{\partial F_M}{\partial v_{\perp}} + \frac{k_{\parallel} V_{\perp}}{\omega v_T^2} F_M + \frac{k_b}{\omega} F_d \right) + i \frac{e}{m} \frac{F_d}{\omega} \frac{\partial(r E_2)}{r \partial r} = \nu_{ef} f_1,$$

$$\omega_c f_1 + i(k_{\parallel} v_{\parallel} - \omega) f_2 + \frac{e}{m} E_2 \left(\frac{\partial F_M}{\partial v_{\perp}} + \frac{k_{\parallel} V_{\perp}}{v_T^2 \omega} F_M \right) - \frac{e}{m} \frac{k_b v_{\perp} E_2}{k_{\parallel} v_{\parallel} - \omega} \left[\frac{\partial v_{\perp} F_d}{2 v_{\perp} \partial v_{\perp}} - \frac{k_{\parallel}}{\omega} \left(\frac{v_{\parallel}}{v_{\perp}} + \frac{V_{\perp}}{2 v_T^2} \right) F_d \right] = \nu_{ef} f_2,$$

where $k_b = MB_z/rB - k_z B_{\theta}/B$, $\omega_{c\alpha} = e_{\alpha} B_0 / m_{\alpha} c$ is the cyclotron frequency, $v_{T\alpha} = \sqrt{T_{\alpha} / m_{\alpha}}$ is the thermal velocity of the plasma species, with index α omitted in above equation. In the cold collision plasma limit ($\nu_e \gg \omega > k_{\parallel} v_{T\alpha}$), the collision integral in the equation for the coefficient f_0 has to be in Landau form, and a solution for this equation is found in Ref. 11 using Chapman-Enskog approach. Another way¹⁰ to calculate the parallel tensor is to solve the fluid equation directly¹² for the parallel velocity. Finally, taking into account electron-ion collisions, the ion rotation velocity \mathbf{V}_i , and an axial cur-

rent density $\mathbf{j} = en_e(\mathbf{V}_e, -\mathbf{V}_i)$ along magnetic surfaces, we have the tensor components

$$\begin{aligned}\varepsilon_{11} &= \varepsilon_{22} \\ &= 1 + \sum_{\alpha=e,i} \frac{\omega_{p\alpha}^2(\omega - \mathbf{k} \cdot \mathbf{V}_\alpha + i\nu_\alpha)(\omega - \mathbf{k} \cdot \mathbf{V}_\alpha - \omega_\alpha^*)}{\omega^2[\omega_{c\alpha}^2 - (\omega - \mathbf{k} \cdot \mathbf{V}_\alpha + i\nu_\alpha)^2]}, \\ \varepsilon_{12} &= -\varepsilon_{21} = i \sum_{\alpha=e,i} \frac{\omega_{p\alpha}^2(\omega - \mathbf{k} \cdot \mathbf{V}_\alpha - \omega_\alpha^*)\omega_{c\alpha}}{\omega^2[\omega_{c\alpha}^2 - (\omega - \mathbf{k} \cdot \mathbf{V}_\alpha + i\nu_\alpha)^2]}, \\ \varepsilon_{33} &= 1 - \sum_{\alpha=e,i} \frac{\omega_{p\alpha}^2}{(\omega - \mathbf{k} \cdot \mathbf{V}_\alpha)(\omega - \mathbf{k} \cdot \mathbf{V}_\alpha + i\nu_\alpha)} \\ &\quad \times \left(1 - \frac{\omega_\alpha^*}{\omega} - 0.71\eta \frac{\omega_\alpha^*}{\omega}\right),\end{aligned}\quad (1)$$

where indexes “1,” “2,” and “3” indicate the radial, binormal, and parallel components, respectively; the drift frequency is defined as $\omega_\alpha^* = (k_b/\omega_{c\alpha}n_\alpha)(\partial/\partial r)(v_{T\alpha}^2n_\alpha)$, with $\eta = d \ln T_e/d \ln n T_e$ for electrons and $\eta=0$ for ions, and n_α is the plasma density.

To understand the results of numerical calculations, we analyze the effect of drift terms in the limit ($E_{\parallel}=0$, and $\nu_i \ll \omega$) in plasmas without ion rotation ($\mathbf{V}_i=0$). For the condition $M^2 \gg N^2 r^2/R_0^2$, the Maxwell equations can be reduced to Hain-Lust equation,^{13,14}

$$\frac{d}{dr} \left[r \left(\varepsilon_{11} \frac{\omega^2}{c^2} - k_{\parallel}^2 \right) \frac{dF}{dr} \right] + F \left[\frac{dg}{dr} - \frac{M^2}{r} \left(\varepsilon_{11} \frac{\omega^2}{c^2} - k_{\parallel}^2 \right) \right] \approx 0, \quad (2)$$

where $F = rE_b$ and $g = M(\omega_{ci}/c_A^2)(\omega_i^* - \omega_e^* - \omega^3/\omega_{ci}^2) + M2k_{\parallel}/R_0q$ come from the ε_{12} -tensor component. Taking the ε_{11} component [Eq. (1)], we have the drift Alfvén continuum¹ $\omega = \omega_i^*/2 \pm \sqrt{(\omega_i^*/2)^2 + k_{\parallel}^2 c_A^2}$. The minimum/maximum of the AW continuum may appear at the rational surface with q -minimum q_r , where k_{\parallel} may be represented as

$$k_{\parallel} \approx \frac{1}{R_0} \left(N + \frac{M}{q_r} - (r - r_m)^2 \frac{Mq''}{2q_r^2} \right). \quad (3)$$

This equation is also valid in the case of negative shear in the plasma core.

Let us consider the possibility of fast drift Alfvén wave excitation due to drift term in the g -function in the LF band $\omega < \sqrt[3]{\omega_{ci}^2(\omega_i^* - \omega_e^*)}$. Generally, fast AW may appear at the plasma core when the functions $D = (\varepsilon_{11}\omega^2/c^2 - k_{\parallel}^2)$ and dg/dr have equal signs. It has been shown numerically¹³ that the global Alfvén wave (named “discrete AW”) appears below the continuum minimum ($D < 0$) due to the Hall effect ω/ω_{ci} for $N/M > 0$ in the high-frequency band. For the LF band and $M/N \approx -q_0$, the Hall effect is very small but the dg/dr function is negative,

$$4M^2 \left(s(s-1) \frac{\beta_0}{a^2} - \frac{(q_a - q_0)}{q_0^3 R_0^2} \right) \frac{r}{a^2} < 0,$$

because of the large last term, where $q = q_0 + (q_a - q_0)r^2/a^2$ is used. The drift part of that function is small for the moderate plasma pressure profile, $p = \beta_0(1 - r^2/a^2)^s B_0^2/4\pi$. In the

plasma core, Eq. (2) can be reduced to Bessel form with the approximate solution

$$F = F_0 J_m(\kappa r); \quad \kappa^2 \approx 4M^2 \frac{q_a - q_0}{q_0 a^2 R_0^2} \left[\frac{c_A^2}{\omega(\omega_i^* - \omega) + k_{\parallel}^2 c_A^2} \right]_{r=0}. \quad (4)$$

That solution is trapped because a nontransparent region appears due to a change of sign, i.e., $dg/dr > 0$, as the radius increases.

For the low shear approximation, i.e., $dk_{\parallel}/dr \approx 0$ and $q \approx -M/N$, we have a positive value for $dg/dr \approx 4s(s-1)\beta_0 M^2 r/a^4 (1 - r^2/a^2)^{s-2} > 0$. In this case, fast drift Alfvén waves may appear in the LF band above the minimum/maximum ($D > 0$) of the AW continuum. In the plasma core, for a moderate pressure profile ($s \geq 2$), an approximate solution of Eq. (2) is the Bessel function

$$F = F_0 J_M \left(\int_0^r \kappa dr \right), \quad (5)$$

$$\kappa^2 \approx 4\alpha(\alpha-1)\beta_0 M^2 (1 - r^2/a^2)^{s-2} \frac{c_A^2}{a^4 [\omega(\omega - \omega_i^*) - k_{\parallel}^2 c_A^2]},$$

where $\kappa^2 a^2 \gg 1$ in the LF band: $\omega \ll \sqrt[3]{\omega_{ci}^2(\omega_i^* - \omega_e^*)} \approx 2\pi(250 \text{ kHz})$.

The solution (5) has to be matched to the solution at the mode conversion point $r = r_A$ ($D = 0$). Expanding the coefficients of Eq. (2) in Taylor series over $x = (r - r_A)/r_A$, we reduce Eq. (2) to Bessel equation of zero index,¹³ which has the solution

$$F = F_1 [J_0(\sqrt{Ax}) + F_2 Y_0(\sqrt{Ax})], \quad A \approx \left[\frac{dg}{dr} \left(\frac{dD}{dr} \right)^{-1} \right]_{r=r_A}. \quad (6)$$

In the low shear case, i.e., $dg/dr > 0$, A is negative due to $dD/dr < 0$. This means that the Bessel and Neumann functions have oscillating profiles for ($x < 0$), which may simplify the matching procedure with the phase $[\int_0^r \kappa dr - (2M+1)\pi/4]$ of the asymptotic solution (5). During a frequency scan when the phase may only match with the J_0 -function in Eq. (6), the LF field can pass through continuum without mode conversion effect or without absorption. We note that changing x from negative to positive in the J_0 -function automatically converts it to the I_0 -function. When the core solution matches only with the Neumann function (Y_0), we have the strong continuum absorption due to the logarithmic divergence of the Y_0 -function that produces the imaginary term $i\pi/2$, when x changes from negative to positive. Finally, an impedance curve should have some periodic oscillation with frequency variation from a minimum to some maximum as it is shown in the calculations.

To calculate the LF fields in the frequency range ($f \leq 150 \text{ kHz}$) with the cylindrical code,⁷ which solves Maxwell equations with the tensor equation (1), an equilibrium cylindrical plasma model is used for the TEXTOR tokamak with circular magnetic surfaces and with simple fitting profiles of plasma parameters: $a = 0.46 \text{ m}$, $R_0 = 1.75 \text{ m}$, b

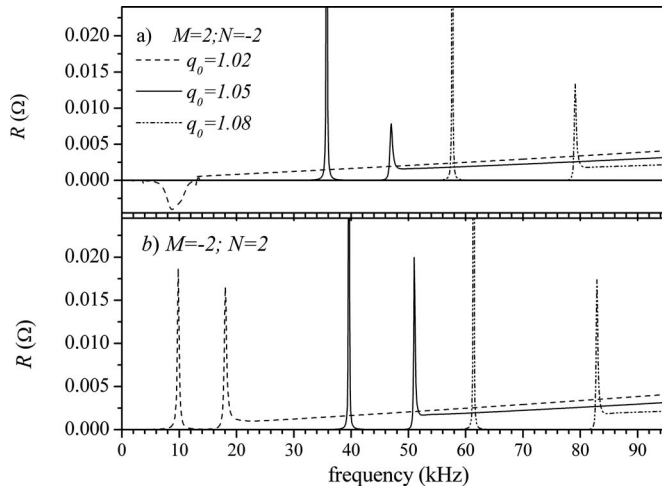


FIG. 1. Plot of the antenna impedances as a function of the frequency for the modes $M/N = \pm 2/\mp 2$ in TEXTOR with $q_a = 4$ and standard q -profile ($q_0 = 1.02, 1.05, 1.08$).

$= 0.5325$ m, $d = 0.6$ m, $B_o(R=R_0) = 2.2$ T, and $I_p = 340$ kA with respect $q_{(r=a)} = q_a = 4.0$. Three cases of the current profile

$$j = \frac{I_p}{\pi a^2} \frac{q(a)}{q(0)} \left[1 + \delta \left(\frac{r}{a} \right)^2 \right] \left[1 - \left(\frac{r}{a} \right)^2 \right]^\gamma$$

are considered: one (named “standard”) for $\delta = 0$, with monotonically growing safety parameter from $q_0 \approx 1.05$ to q_a ; another with quasiflat shear profile ($\delta = 2.3$, $\gamma = 2.2$), where $q_0 = 1.92$; and another one with negative shear profile where $q_0 = 2.03$ ($\delta = 3.5$, $\gamma = 2.5$). The ion rotation $\mathbf{V}_i = 0$ is used in the calculations. Parabolic temperature profiles are considered: $T_i = 1110[1 - (r/a)^2]^2 + 90$, and $T_e = 1940[1 - (r/a)^2]^2 + 60$ eV for ions and electrons, respectively. The density profile is taken as $n_e = n_0\{[1 - (r/a)^2] + 0.03\}$, with $n_0 = 3 \times 10^{19} \text{ m}^{-3}$. To calculate the absorbed power density, we use the standard definition $W = \langle \mathbf{j} \cdot \mathbf{E} \rangle$. Furthermore, the coil impedance, which is total absorbed power normalized to half of the coil current square is calculated for TEXTOR parameters. In the case of negative shear, using the dimensionless parameter $\beta_0 R_0^2/a^2 = \text{const}$, we simulate the conditions of the Test Fusion Tokamak Reactor (TFTR) experiment³ for the TEXTOR parameters.

For the standard shear profile, the antenna impedances of the $M/N = \pm 2/\mp 2$ modes are shown for $q_0 = 1.02, 1.05$, and 1.08 in Fig. 1. Double spikes are related to the global resonances for two different radial wave numbers. The real part of the E_r -component of the LF field for the first spikes of the $M/N = \pm 2/\mp 2$ modes is presented in Fig. 2. Those sharp spikes and E_r -field distribution are typical for the global AW resonances,¹⁵ as is discussed in the theory section. The negative spike for $q_0 = 1.02$ in Fig. 1(a), with $f \approx 9$ kHz, appears below the specific drift frequency $f_{se}^* \approx 1.71 f_e^*$ for the electrons. This effect is produced by changing of the imaginary part of the ϵ_{33} -component of the dielectric tensor that reflects the instability condition of the electron drift wave. We note that other global AW resonances also appear for the other poloidal/toroidal modes $M = -N > 0$.

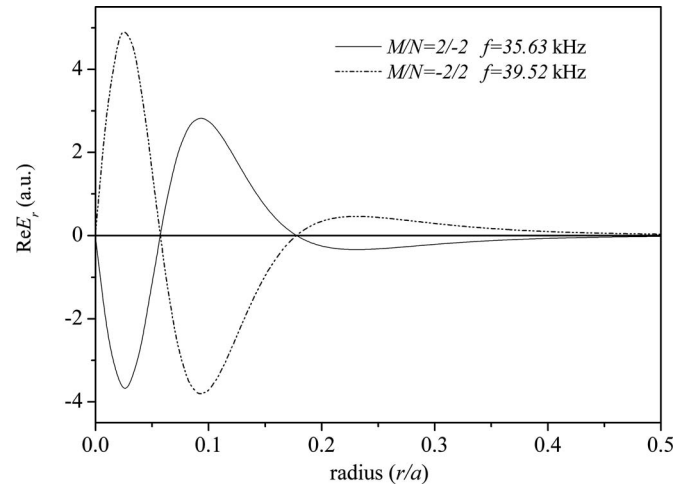


FIG. 2. Real part of the E_r -field for the $M/N = (2/-2)$ (solid line), $M/N = (-2/2)$ (dash-dot-dot line) modes over the normalized radius in the first spike for $q_0 = 1.05$ of Fig. 1.

Next, we analyze the LF wave excitation in the AW continuum for the flat and negative shear profiles shown together with electron drift frequency in Fig. 3(a). The respective antenna impedance for $M/N = 2/-1$ is presented in Fig. 3(b). The impedance behavior is characterized as oscillating from a minimum to some maxima, which increase with frequency. The last maxima (not shown) have frequency 159 kHz for the negative profile and 146 kHz for the flat shear. To compare the behavior of LF fields in maximums and minimums of the impedance, the imaginary part of the E_r -component and absorption of LF fields for $M/N = 2/-1$ are plotted in Figs. 4(a) and 4(b). For the frequency $f = 37.5$ kHz in flat shear impedance maximum, we observe in Fig. 4(a) that the LF field absorption is concentrated at the AW continuum position of the $M/N = 2/-1$ modes and there is an oscillating E_r -field structure related to fifth radial mode number. Contrary to that, in the impedance minimum with the frequency

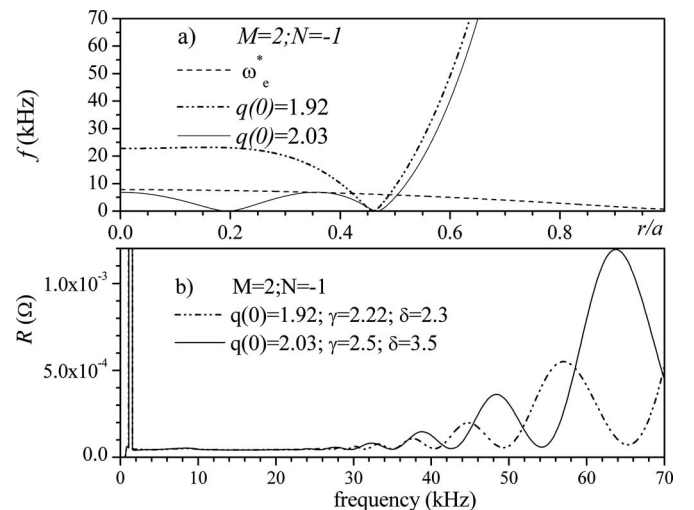


FIG. 3. Plot of the specific electron drift frequency and Alfvén wave continuum over radius (a) and antenna impedance (b) as function of the frequency for the modes $M=2, N=-1$ in TEXTOR with negative (solid) and flat shear profile (dash-dot-dot line).

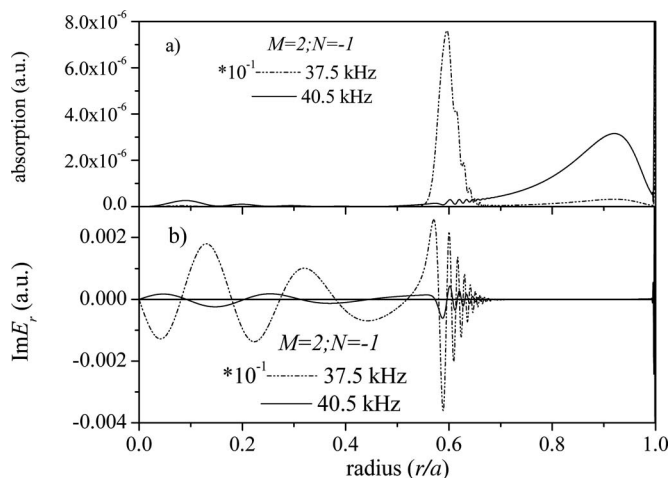


FIG. 4. Absorbed power (a) and imaginary part of the radial electric field (b) over the normalized radius for the $M/N=(2/-1)$ mode in the minimum (solid line, $f=40.5$ kHz) and the maximum (dashed line, $f=37.5$ kHz) of the impedance in Fig. 3.

$f=40.5$ kHz, the LF field absorption with the same radial mode number is absent at the AW continuum position this result is in good agreement with the theory section. The same behavior of the LF fields and absorption is found for negative shear at minimum/maximum of the impedance.

Finally, taking into account the q -profile and diamagnetic drift effect in the calculations of the power absorption and low-frequency electromagnetic fields driven by a helical antenna or ergodic dynamic divertor in the tokamaks, we conclude that:

- Nonpotential fast Alfvén waves with small k_{\parallel} can be effectively excited in the low-frequency band of tokamak plasmas even in the presence of the Alfvén continuum.
- The dispersion of the fast waves depends on the q -profile and on the derivative of the diamagnetic drift terms; for the standard tokamak shear the fast drift Alfvén waves (as glo-

bal Alfvén waves) are excited in the plasma core below the Alfvén continuum minimum with $q_0 \approx (-N/M)$ that is slightly larger than 1.

- High sensitivity of that global resonance from the central q -value may simplify the experimental definition of q_0 , which is relevant for tokamak stability.
- For the negative (or flat) shear profile in the plasma core, the fast waves dispersion above the Alfvén continuum minimum is defined by the derivative of the drift terms and the continuum may be transparent, depending on the phase of these waves.

This work was supported by FAPESP (Research Foundation of the State of São Paulo) and by CNPq (National Council of Scientific and Technological Development), Brazil.

¹A. B. Mikhailovskii, in *Reviews of Plasma Physics*, edited by M. A. Leontovich (Consultants Bureau, New York, 1967), Vol. 3, p. 159.

²W. Horton, *Rev. Mod. Phys.* **71**, 735 (1999).

³F. M. Levinton, M. C. Zarnstorff, S. H. Batha, M. Bell, R. E. Bell, R. V. Bundy, C. Bush, Z. Chang, E. Fredrickson, A. Janos, J. Manickam, A. Ramsey, S. A. Sabbagh, G. L. Schmidt, E. J. Synakowski, and G. Taylor, *Phys. Rev. Lett.* **75**, 4417 (1995).

⁴K. H. Burrell, *Phys. Plasmas* **4**, 1499 (1997).

⁵Ph. Ghendrih, A. Grossman, and H. Capes, *Nucl. Fusion* **42**, 1221 (2002).

⁶K. H. Finken, S. S. Abdullaev, W. Biel *et al.*, *Plasma Phys. Controlled Fusion* **46**, B143 (2004).

⁷E. R. Rondan, A. G. Elfimov, R. M. O. Galvão, and C. J. A. Pires, *Nucl. Fusion* **46**, S154 (2006).

⁸M. F. Heyn, I. B. Ivanov, S. V. Kasilov, and W. Kernbisher, *Nucl. Fusion* **46**, S159 (2006).

⁹A. G. Elfimov, C. A. de Azevedo, A. S. de Assis, N. I. Grishanov, F. M. Nekrasov, I. F. Potapenko, and V. S. Tsypin, *Braz. J. Phys.* **25**, 224 (1995).

¹⁰V. S. Tsypin, A. G. Elfimov, and R. M. O. Galvão, *Phys. Plasmas* **14**, 014503 (2007).

¹¹A. F. Alexandrov, L. S. Bogdankevich, and A. A. Rukhadze, *Principles of Plasma Electrodynamics* (Springer-Verlag, Berlin, 1984).

¹²S. I. Braginskii, *Reviews of Plasma Physics*, edited by M. A. Leontovich (Consultants Bureau, New York, 1965), Vol. 1, p. 205.

¹³A. G. Elfimov, *Sov. Phys. JETP* **10**, 405 (1984).

¹⁴J. P. Goedbloed and H. J. Hagebeuk, *Phys. Fluids* **15**, 1090 (1972).

¹⁵D. W. Ross, G. L. Chen, and S. M. Mahajan, *Phys. Fluids* **25**, 652 (1982).